

cy. 2



## AEROBALLISTIC RANGE INSTRUMENTATION DEVELOPMENT

VON KÁRMÁN GAS DYNAMICS FACILITY  
ARNOLD ENGINEERING DEVELOPMENT CENTER  
AIR FORCE SYSTEMS COMMAND  
ARNOLD AIR FORCE STATION, TENNESSEE 37389

September 1976

Final Report for Period July 1972 – June 1975

Approved for public release; distribution unlimited.

Property of U. S. Air Force  
AEDC LIBRARY  
F40600-75-C-0001

Prepared for

DIRECTORATE OF TECHNOLOGY (DY)  
ARNOLD ENGINEERING DEVELOPMENT CENTER  
ARNOLD AIR FORCE STATION, TENNESSEE 37389

## NOTICES

When U. S. Government drawings specifications, or other data are used for any purpose other than a definitely related Government procurement operation, the Government thereby incurs no responsibility nor any obligation whatsoever, and the fact that the Government may have formulated, furnished, or in any way supplied the said drawings, specifications, or other data, is not to be regarded by implication or otherwise, or in any manner licensing the holder or any other person or corporation, or conveying any rights or permission to manufacture, use, or sell any patented invention that may in any way be related thereto.

Qualified users may obtain copies of this report from the Defense Documentation Center.

References to named commercial products in this report are not to be considered in any sense as an endorsement of the product by the United States Air Force or the Government.

This report has been reviewed by the Information Office (OI) and is releasable to the National Technical Information Service (NTIS). At NTIS, it will be available to the general public, including foreign nations.

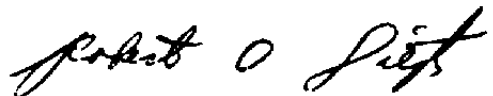
## APPROVAL STATEMENT

This technical report has been reviewed and is approved for publication.

FOR THE COMMANDER



MARSHALL K. KINGERY  
Research & Development  
Division  
Directorate of Technology



ROBERT O. DIETZ  
Director of Technology



# UNCLASSIFIED

## 20. ABSTRACT (Continued)

bow shock waves on certain test models. Model detector systems have been developed and have demonstrated a 93-percent trigger reliability when used in the high-luminosity, blast-tank area of Hyperballistic Range (K); reliability of previously used systems was 70 percent. Other evaluations have shown that high reliability can be expected in applications of these types of detectors for triggering instrumentation systems in the Range K and Range G guided-track facilities.

## PREFACE

The work reported herein was conducted by Arnold Engineering Development Center (AEDC), Air Force Systems Command (AFSC), under Program Element 65807F. The results were obtained by ARO, Inc. (a subsidiary of Sverdrup & Parcel and Associates, Inc.), contract operator of AEDC, AFSC, Arnold Air Force Station, Tennessee. The research was done under ARO Project Numbers VF201, VF401, and V32S-38A. The author of this report was Paul H. Dugger, ARO, Inc. The manuscript (ARO Control No. ARO-VKF-TR-75-84) was submitted for publication on June 20, 1975.

The author acknowledges the contributions of Messrs. O. H. Bock, C. P. Enis, B. W. Gilley, H. G. Harris, and J. W. Hill, Instrumentation Engineers of the von Kármán Gas Dynamics Facility (VKF), who performed the bulk of experimental work of the program. The author also wishes to thank Mr. R. E. Hendrix, Supervisor of the Range Instrumentation Section, VKF, for his helpful suggestions throughout the program and for his critical review of the manuscript.

## CONTENTS

	<u>Page</u>
1.0 INTRODUCTION . . . . .	5
2.0 PHOTOGRAPHIC PYROMETRY	
2.1 "Low" Temperature Photopyrometers . . . . .	6
2.2 Shock-Cap Air Radiation . . . . .	7
2.3 Dual-Environment Technique . . . . .	9
2.4 "Low" Temperature Measurements . . . . .	9
2.5 Qualitative Application . . . . .	12
3.0 HIGH-SPEED SEQUENTIAL PHOTOGRAPHY SYSTEM	
3.1 Camera . . . . .	13
3.2 Framing Rate Requirements . . . . .	13
3.3 Light Source . . . . .	14
3.4 Optical System . . . . .	16
3.5 Photographic Results . . . . .	17
4.0 MUZZLE-ZONE/TRACK DETECTOR SYSTEMS	
4.1 System Description . . . . .	20
4.2 Operational Characteristics . . . . .	20
4.3 Evaluations . . . . .	21
5.0 CONCLUDING REMARKS . . . . .	22
REFERENCES . . . . .	23

## ILLUSTRATIONS

Figure

1. Aeroballistic Range G Photographic Pyrometer System . . . . .	6
2. Temperature Error Induced by Shock-Cap Air Radiation, Approximate Calculations . . . . .	8
3. Noretip Transition Test Model . . . . .	10
4. Isothermal Contours on Graphite Model Noretip . . . . .	11
5. Self-Luminosity Photograph of Hypervelocity Model and Wake . . . . .	12
6. Flashlamp Electronics . . . . .	15
7. Light Output Pulses from FT-230 Flashtube . . . . .	16

<u>Figure</u>	<u>Page</u>
8. High-Speed Photography System for Erosion Studies . . . . .	17
9. Typical Frame from High-Speed Photography System, Snow Erosion Studies . . . . .	18
10. Typical Frame from High-Speed Photography System, Flow Visualization Mode . . . . .	19
11. Detector System Schematic . . . . .	20

## 1.0 INTRODUCTION

In order to ensure against obsolescence of the aeroballistic ranges of the von Kármán Gas Dynamics Facility (VKF) as practical ground test facilities, it is essential to develop and expand instrumentation systems to meet the imposed data acquisition requirements as areas of testing change or become more sophisticated. Experimental research programs for this express purpose have been in effect for the past several years. The results from past projects are presented in Ref. 1. The purpose of this report is to describe some instrumentation systems developed and evaluated under the ensuing research projects.

## 2.0 PHOTOGRAPHIC PYROMETRY

Photographic pyrometry systems have been developed within the VKF and have demonstrated the capability for measurements of temperatures on the surfaces of models in flight at velocities as high as 20,000 ft/sec in Hyperballistic Range (G). The technique involves basically the following sequence: (1) A high-speed image intensifier camera is used to obtain a stop-motion, self-luminosity photograph of the model in flight. Exposure times as short as 10 nsec can be obtained with the image intensifier systems. (2) Calibrations from a carbon-arc reference source are recorded on identical film and are processed simultaneously with the model photograph. (3) Densities of the film image of the model surface are measured (via a scanning microdensitometer) and converted to temperatures using the densities likewise extracted from the calibration data. The temperatures thus measured are brightness temperatures and may be converted to true surface temperatures provided that, first, the luminosity recorded is strictly incandescent in nature, and secondly, the emissivity of the model material is known.

The photographic pyrometry technique used in Range G is represented schematically in Fig. 1. The geometry of this arrangement provides matched optical paths for system calibration and data acquisition. The recording camera consists of an objective lens, an image intensifier device, a relay lens or fiber-optics faceplate, and a combination ground-glass and film holder. In-depth descriptions and discussions of these photographic pyrometer systems can be found in Refs. 1 through 5.

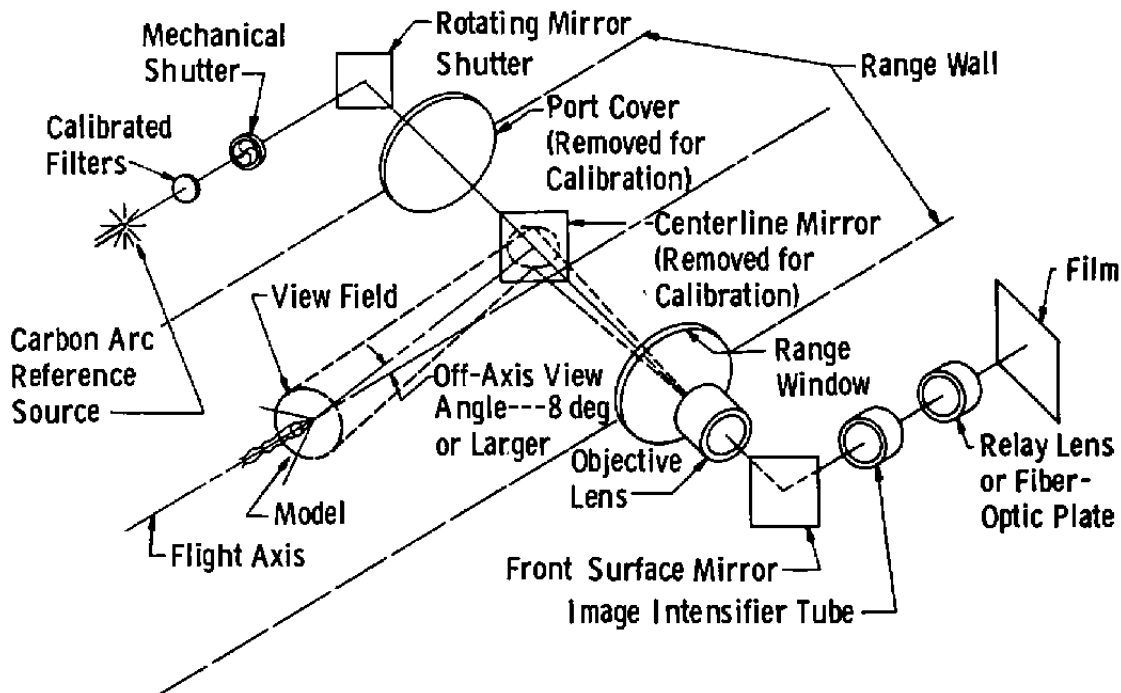


Figure 1. Aeroballistic Range G photographic pyrometer system.

## 2.1 "LOW" TEMPERATURE PHOTOPYROMETERS

It has been a goal of the sequence of these research projects to extend the lower measurement limit of Range G photopyrometry systems. The initial systems (Refs. 1 through 5), developed for and used quite successfully during ablation and erosion testing, cannot make reliable surface temperature measurements below about 2,500 K\*. Certain other areas of testing require measurements of temperatures which fall below the measurement range of these systems.

The primary component in the photopyrometry technique described above is, of course, the image intensifier device, and the overall sensitivity of the photopyrometer to temperature is determined, to a large extent, by the spectral response of the image intensifier. The image intensifiers used in the initial Range G photopyrometers have S-11 spectral response characteristics; i. e., these devices respond to radiation within the spectral band from 0.35 to 0.65  $\mu\text{m}$ , approximately. The incandescent radiation from the aerodynamically heated model

---

\*"Low" is used herein to describe temperatures in the regime below 2,500 K.

surfaces is governed by the familiar Wien Displacement Law,  $\lambda_{\max} T = 2898 \mu\text{m K}$ , where  $\lambda_{\max}$  is the wavelength at which the radiation curve peaks for a surface at temperature T. Obviously then, the capability for detection of longer wavelength radiation should allow measurements of lower temperatures.

Recent advances in the state-of-the-art of image intensifier devices have made available a proximity-focused, fiber-optics-coupled, image intensifier diode with a spectral response designated S-20R that extends into the near infrared; the device responds within the spectral band from 0.35 to 0.93  $\mu\text{m}$ . Also, the diode has high sensitivity and can be gated at nanosecond times, making it suitable for the aeroballistic range application. Analytical studies were made indicating that utilization of one of these state-of-the-art diodes in a photopyrometry system should allow measurements of surface temperatures as low as approximately 1,850 K.

A photopyrometry system was designed around a diode manufactured by Galileo (formerly, Bendix) Electro-Optics, Inc. The system, including power supply, camera housing, etc. (see Fig. 1), was constructed and was evaluated in the laboratory. It was found through observations of a calibration source that the system was indeed capable of temperature measurements as low as 1,800 K under the static laboratory conditions.

## 2.2 SHOCK-CAP AIR RADIATION

When making aeroballistic range surface temperature measurements via the photopyrometry technique, one must not only be concerned with the measuring instrument, but must also carefully consider the radiating characteristics of the source being measured; i. e., it must be ascertained that only incandescent radiation from the model surface is seen by the photopyrometer. Several possible sources of extraneous radiation are discussed in Ref. 2. The one of these of major concern for the measurements of interest is felt to be that of shock-cap air radiation.

Studies were made wherein it was approximated, for example, that the shock-cap radiation (at the stagnation point), characteristic of a 0.5-in. nose radius model in flight at 15,000 ft/sec in a range pressure of 200 torr (air), has a brightness temperature of 2,000 K, as might be seen by an S-20R response photopyrometer; i. e., the air radiation would elicit the same response from the particular photopyrometer as would a

2,000 K blackbody surface. Clearly then, the air radiation would influence measurements of surface temperature in the region of interest (<2,500 K), and measurements of temperatures lower than 2,000 K would not be possible in the presence of the radiating air. The temperature measurement errors that would be caused by the extraneous radiation for this example case are illustrated in Fig. 2. Fortunately, since blackbody radiation is such a strong function of temperature\*, the effects of air radiation diminish quite rapidly for surface temperatures higher than the brightness temperature of the excited air (see Fig. 2). At temperatures encountered during ablation and erosion testing (typically greater than 3,500 K), the errors caused by air radiation are insignificant.

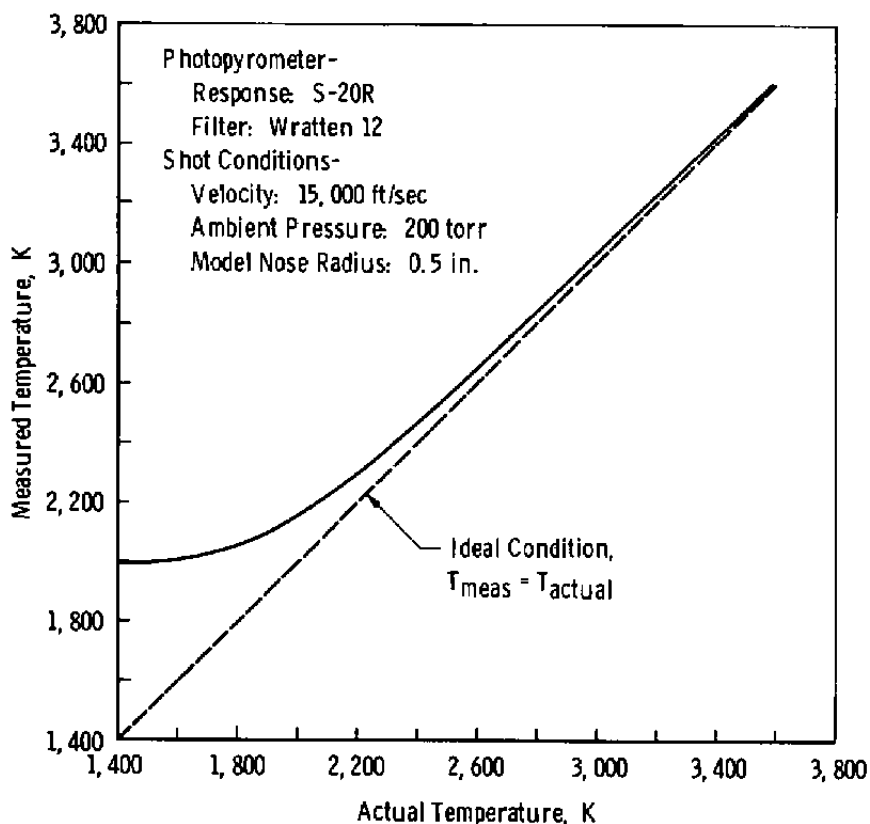


Figure 2. Temperature error induced by shock-cap air radiation, approximate calculations.

\*It is well known that, for a blackbody at temperature  $T$ , the total radiation is proportional to  $T^4$ . However, within the wavelength band defined by the S-20R response and at the temperatures pertinent to this discussion, the radiation varies considerably more rapidly (than  $T^4$ ) with temperature.

### 2.3 DUAL-ENVIRONMENT TECHNIQUE

Obviously, if reliable temperature measurements at levels below 2,500 K are to be made, the only feasible approach is to remove the influence of the shock-cap air radiation\*. A scheme was devised whereby this might be accomplished in Range G to allow meaningful evaluation and use of the "low" temperature photopyrometer. The scheme involves flying the test model into an evacuated (very low pressure) section of the range immediately prior to making the photopyrometer temperature measurements. The "low" temperature photopyrometer was installed just downrange from a bulkhead/quick-opening valve system that is located approximately 310 ft from the range entrance. This bulkhead/valve system allowed separation of the flight path into two pressure environments. Pressures in the uprange portion could be chosen to simulate the desired reentry test conditions (typically, 100 to 300 torr), while the downrange portion could be pumped down to about 1 torr. The quick-opening valve could be utilized to maintain separation of these two pressure environments until a few milliseconds prior to arrival of a model.

The "low" temperature photopyrometer was arranged so that a test model could be viewed at an axial location approximately 20 ft downrange from the bulkhead. During testing, then, flight times from entry through the portal of the quick-opening valve into the low pressure until arrival at the photopyrometer view field were on the order of 1.1 msec. These times are felt to have been sufficient for quenching of shock-cap radiation and yet to have been short enough that the test model surfaces, aerodynamically heated during flight in the simulated reentry environment, could not cool by any appreciable amount prior to the temperature measurements.

### 2.4 "LOW" TEMPERATURE MEASUREMENTS

The "low" temperature photopyrometer was used as a primary data system during a SAMSO Noretip Transition Test (V41G-09A) in Range G. Actually, development of the "low" temperature measurement capability was a prerequisite for performing this test program, since the desired test conditions were such that surface temperatures would be too low to be measured with the original Range G photopyrometers. Test objectives were compatible with the limitations of the dual-environment technique (i. e., a single measurement station and the foreshortened test environment, 310 ft).

---

\*Calculations of brightness temperatures for shock-cap radiation, as in the example, are much too approximate to allow mathematical removal of such effects.

Figure 3 is a photograph illustrating the hemisphere/cylinder/cone test models used for the nosetip transition tests. The hemispherical tip is graphite and has a diameter of 1 in. Figure 4 shows an isothermal contour map of nosetip temperatures measured with the "low" temperature photopyrometer during one of the launches; these data were taken at an aspect angle approximately 10 deg from head-on. The model velocity was 18,400 ft/sec, the range pressure in the up-range section was 116 torr, and the pressure in the downrange section was 1 torr. Computer-generated indications of surface contours for the obliquely viewed hemispherical nosetip have been superimposed on the isothermal map in Fig. 4 to aid in visualization and interpretation; these are represented by the curved lines and dotted rings.

The temperature data in Fig. 4 are typical of those obtained with the new photopyrometer throughout the test; 1,900 K contours were measured on a few shots. Apparently, the dual-environment technique does provide a means for circumventing shock-cap radiation problems. Certainly one would expect shock-cap radiation, if present,

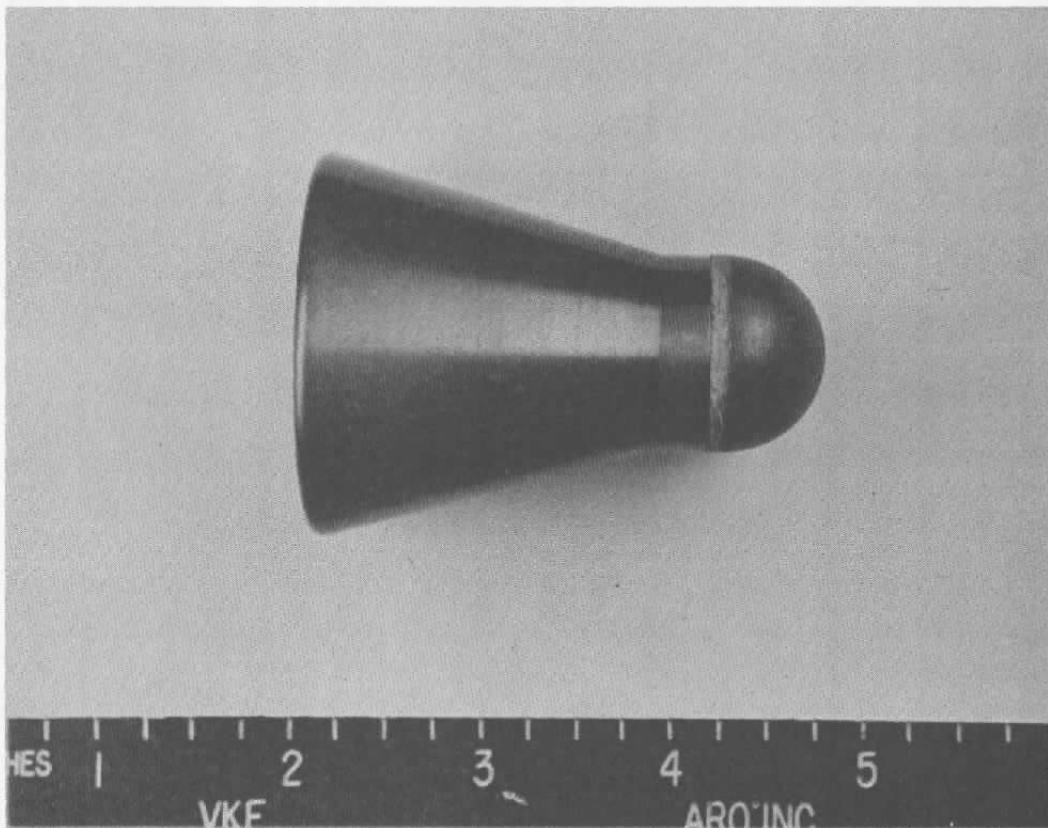
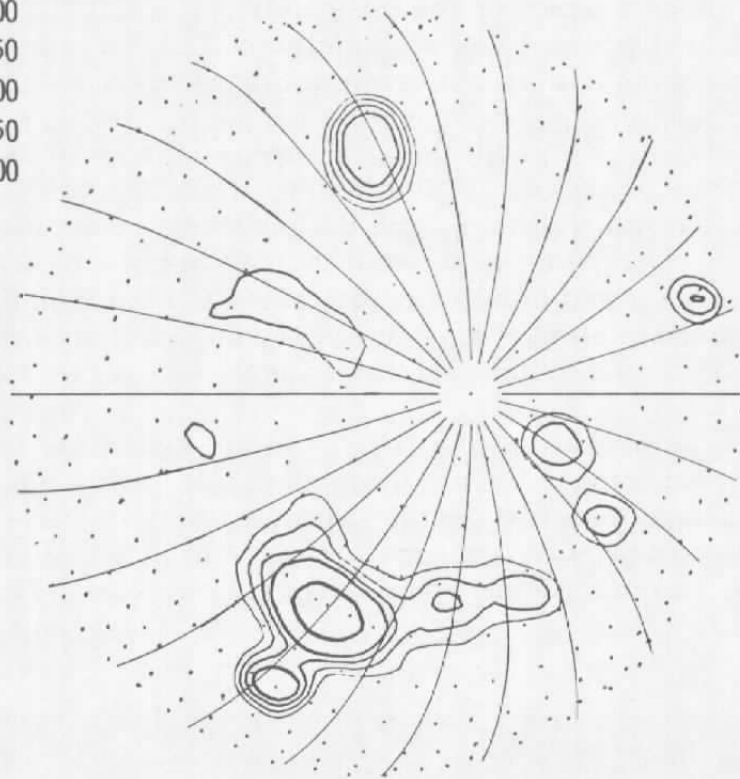


Figure 3. Nosetip transition test model.

<u>Sym</u>	<u>Temperatures, K</u>
—	2300
—	2150
—	2100
—	2050
—	2000



- Notes: 1. Instrumentation System: "Low" Temperature Photopyrometer, Exposure Time: 100 nsec  
 2. Nosetip Diameter: 1 in.  
 3. Model Velocity: 18,400 ft/sec  
 4. Surface contours of the obliquely viewed hemispherical nosetip are indicated by dots and curving lines.

**Figure 4. Isothermal contours on graphite model nosetip.**

to be maximum at the stagnation point; whereas, all temperature data recorded during the test were characterized by an absence of any measurable radiation from the stagnation point region, as typified by Fig. 4.

The lower measurement limits of previous Range G photopyrometers would have precluded acquisition of any of the temperature data in Fig. 4 and most of that during the entire transition test. Clearly then, development of the new "low" temperature instrumentation system has extended the testing capability for Range G.

The "low" temperature photopyrometer has an upper measurement limit approximately the same as the previous photopyrometers (typically, 4,500 K). This increased dynamic range is, of course, a highly desirable feature and will permit use of the device during ablation and erosion testing, for example, as well as in "low" temperature measurement applications.

## 2.5 QUALITATIVE APPLICATION

Use of the "low" temperature photopyrometer system as a device for obtaining important qualitative data was demonstrated. During one aeroballistic range test series, it was of interest to observe the luminous wakes behind hypervelocity models. The photopyrometry system was changed to afford a broadside viewing angle and was operated in a photograph-only mode (i. e. , with no temperature calibration) at exposure times of 1  $\mu$ sec. The resulting self-luminosity photographs do indeed provide excellent depictions of the wakes; Fig. 5 shows one of these photographs. It should be pointed out that temperature data cannot be extracted from the photographs because the radiation is not incandescent.

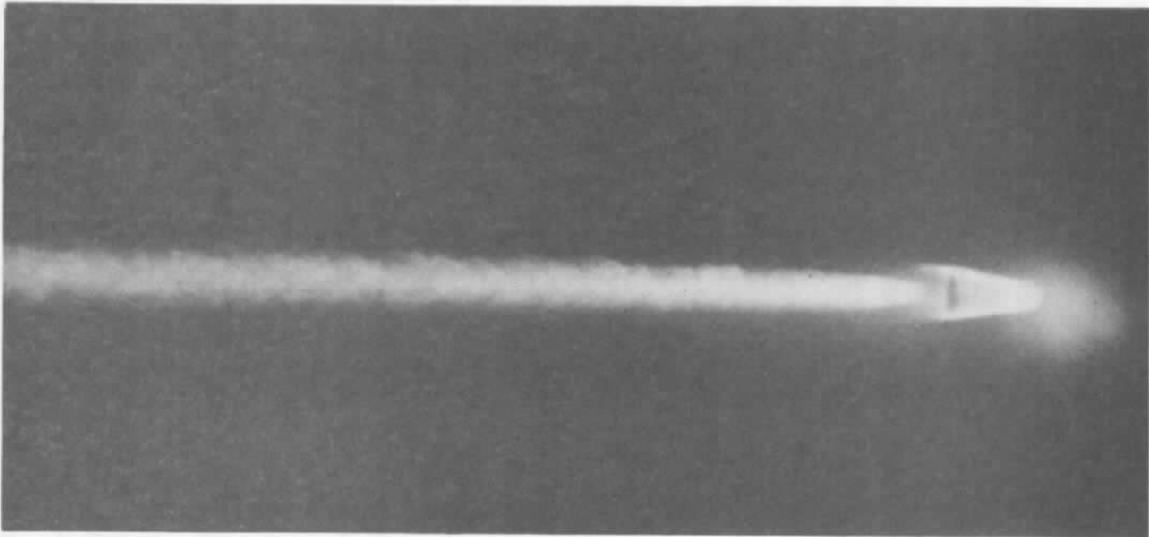


Figure 5. Self-luminosity photograph of hypervelocity model and wake.

## 3.0 HIGH-SPEED SEQUENTIAL PHOTOGRAPHY SYSTEM

Requirements for a high-speed sequential photography system arose in two areas of testing in Range G. First, it was desirable

during erosion testing to record the flights of test models through snowfield environments for the purpose of studying snowflake/shockwave interactions. Secondly, inquiries regarding future testing indicated interest in observing and measuring the oscillatory frequency of bow shock waves on certain types of sharply pointed test models. It was decided that a system that would fulfill both these requirements could be developed around an available Beckman & Whitley, Model 192, continuous-writing framing camera.

### 3.1 CAMERA

The Beckman & Whitley Model 192 is a turbine-driven, rotating-mirror, high-speed framing camera capable of operation at framing rates up to 1,440,000 frames per second (fps). The total recording time at the maximum framing rate is 55  $\mu$ sec; total recording time is correspondingly longer for lower framing rates. An 82-picture record is placed on two separate lengths of 35-mm film, with adjacent frames separated by equal time increments. The camera is continuous writing, i. e., the camera is brought to its preselected operating speed and continuously sweeps through the 82 frame locations. The event to be recorded may begin at any time\* after the camera reaches operating speed but must not have a duration greater than the total recording time for the selected camera speed. An event longer than the recording time will result in rewriting -- an "eighty-third" picture will be doubly exposed on the "first" picture, etc.

In the aeroballistic range application, there can be no electronic control over the "event" proper -- it simply consists of the passage of the test model through the camera's field of view, and its duration is determined by the test velocity and view field; the test velocity, of course, is defined by test objectives and cannot be chosen to suit the camera. Thus, one must control the period of time that the event is illuminated to avoid the rewriting conditions.

### 3.2 FRAMING RATE REQUIREMENTS

For observing the penetration of a snowfield by a hypervelocity test model, it is desirable to record a sequence of photographs, with one-fourth to one-half inch of model travel transpiring between photographs (frames). Model velocities used in erosion testing are normally within the 12,000- to 19,000-ft/sec range. A framing rate of

---

\*The "first" picture may occur at any one of the 82 frame locations.

500,000 fps was chosen as a design criterion for this application. This framing rate corresponds to a time interval of  $2 \mu\text{sec}$  between frames. Model travel between frames, then, would be approximately 0.29 in. at 12,000 ft/sec up to approximately 0.46 in. at 19,000 ft/sec. The optimum duration of a light source for use with the camera operating at 500,000 fps would be 82 frames/500,000 fps or  $164 \mu\text{sec}$ . Exposure time per frame would be approximately  $0.5 \mu\text{sec}^*$ .

Based on the predictions of investigators interested in observing oscillating bow shock waves, it was determined that a framing rate of 1,000,000 fps would be required to record a sufficient number of incremental progressions for characterization of these cyclic phenomena. This  $10^6$ -fps framing rate would then require a light source with a duration of  $82 \mu\text{sec}$  (82 frames/ $10^6$  fps) for optimum photographic capability; exposure time per frame would be approximately  $0.25 \mu\text{sec}$ .

### 3.3 LIGHT SOURCE

The major problem associated with application of the high-speed camera concerned provision of a light source to meet the time-duration requirements outlined in Section 3.2, above. In addition, as one might expect, a high intensity source is required to give adequate film exposures during the short exposure times --  $0.5$  or  $0.25 \mu\text{sec}$  per frame.

Ideally, the light source should come on instantaneously as a model enters the field of view, maintain a constant, high-intensity level while the camera records the 82 frames of information, then instantaneously shut off to avoid rewriting. This ideal "square wave" case, recognized as impossible to achieve in practice, was the design goal.

A General Electric, Type FT-230 flashtube (Ref. 6) was chosen as the basic element of the lighting system. This flashtube is a short-gap, high-intensity, xenon-filled tube and is capable of operation at the short durations desired. Operating voltage requirements for this flashtube are on the order of 2.5 kv; the output light pulse follows very closely the input current pulse.

A suitable pulse-forming network for supplying the high-voltage, high-speed pulses to the flashtube could not be located commercially; therefore, it was necessary to design and fabricate this item in-house.

---

\*For the internal optical configuration of this particular camera, the exposure time is approximately one-fourth the time between frames.

A schematic diagram of the flashtube electronics, as designed, is shown in Fig. 6. The basic circuit is, in electronic terminology, a modified, Type E delay line. A detailed analysis of the circuitry will not be given here; however, it is of interest to point out the effects of the addition of "crowbar" spark gaps to the basic delay line. Actually, it is this innovation that makes the circuit applicable for providing the desired light output pulses.

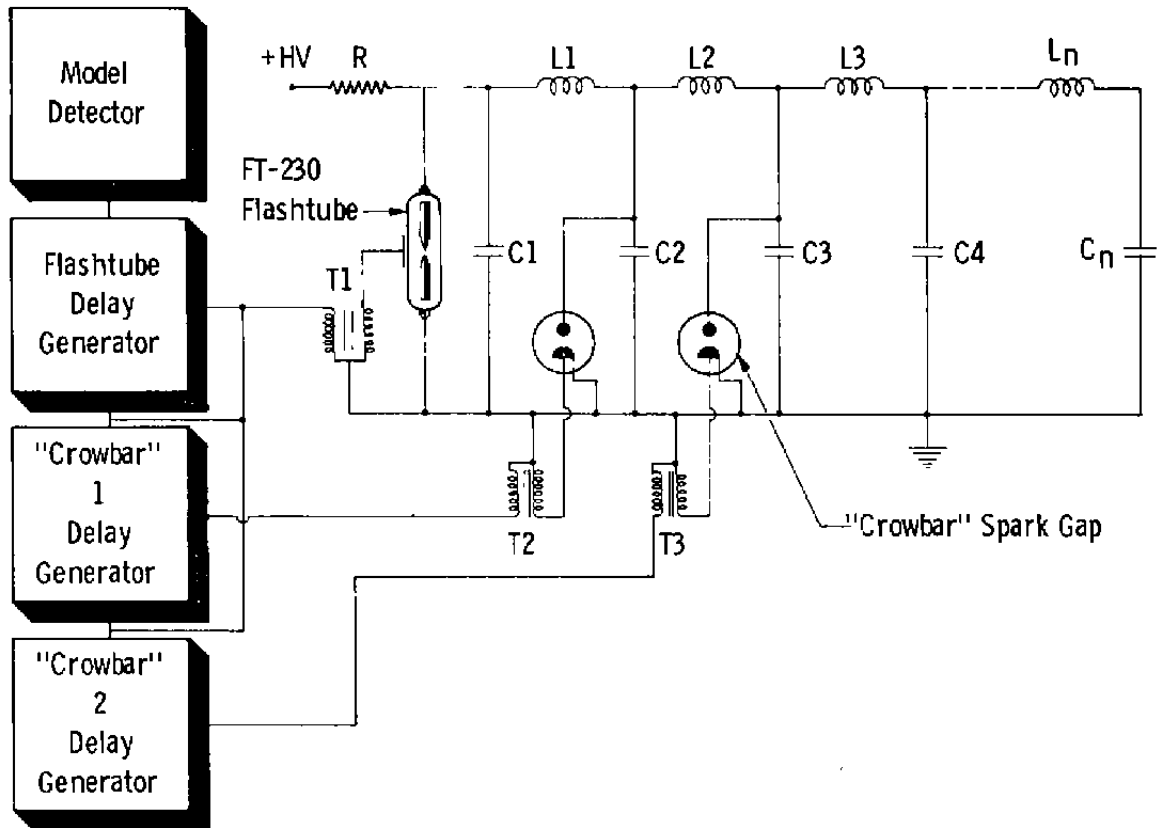


Figure 6. Flashlamp electronics.

Because of an impedance mismatch between the flashtube (after triggering) and the pulse-forming network, reflected waves occur in this network and are manifested in the light output traces. Figure 7a illustrates a light output pulse from the system without the "crowbar" spark gaps; this particular occurrence was encountered during attempts to produce the approximately 80- $\mu$ sec light pulse necessary for  $10^6$ -fps camera operation. As a result of the reflected waves, the desired pulse of approximately 80  $\mu$ sec is followed by undesirable residual pulses. Activation of the "crowbar" spark gaps at the properly chosen times

effectively short-circuits capacitor voltage and removes the residual pulses as is evidenced by Fig. 7b, thus leaving a reasonably "square" pulse\*. For this particular case, the pulse width is approximately 70  $\mu$ sec at the 1/3-peak points. Recalling that, for  $10^6$ -fps camera operation, rewriting will begin after approximately 80  $\mu$ sec, it can be seen from Fig. 7b that a small amount of lighting (approximately 15 percent of maximum) will persist when rewrite begins. It has been shown during operation of the camera that this rewrite condition is barely perceptible in the photographs and does not seriously affect the photographic quality. The circuitry illustrated in Fig. 6 was also used, with certain modifications, to produce reasonably "square" light pulses of approximately 160  $\mu$ sec duration for the 500,000-fps, model/snowfield photography application.

Vertical Scale: Relative Intensity  
Horizontal Scale: Time (20  $\mu$  sec/large division)

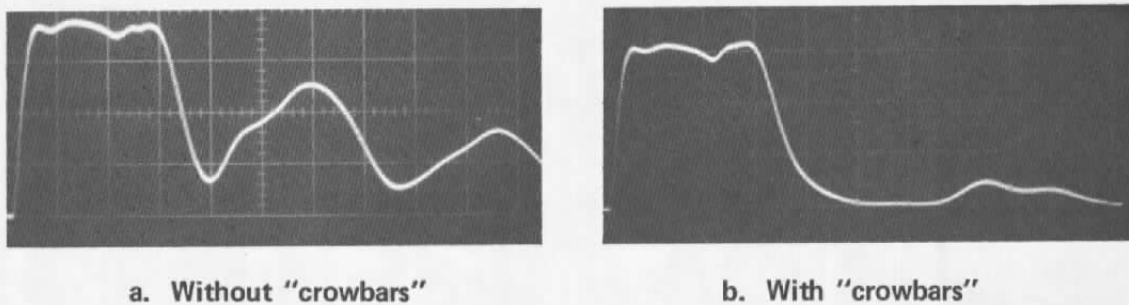


Figure 7. Light output pulses from FT-230 flashtube.

### 3.4 OPTICAL SYSTEM

Adaptation and installation of the high-speed photography system for use in Range G was straightforward. A backlight arrangement was chosen for both applications (snowfield and shock-wave photography).

The arrangement for snowfield photography is depicted in simplified form in Fig. 8. Light from the high-intensity light source (with circuit configuration such as to produce approximately 160- $\mu$ sec pulses) is directed by a 15-in.-diam, 65-in.-focal length lens across the desired viewfield and into the framing camera. Diameter of the field of view at

---

\*The amplitude of the input voltage pulse for this case 2.6 kv.

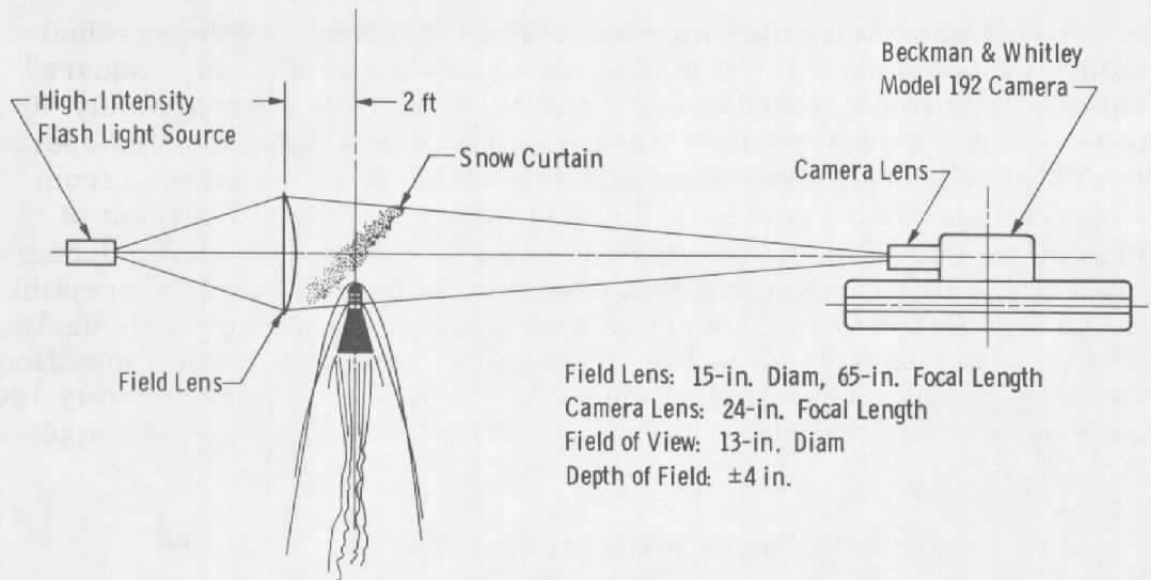


Figure 8. High-speed photography system for erosion studies.

range centerline is approximately 13 in. The camera lens (24-in. focal length) is focused on the range centerline; depth of field is such as to allow approximately  $\pm 4$  in. of model dispersion without serious degradation of photographic quality.

Components used in the range installation but not shown in the simplified schematic of Fig. 8 include a pair of front-surface mirrors to fold and direct the light beam into the range and onto the field lens, and a second pair of front-surface mirrors to direct the beam into the camera. The Beckman & Whitley Model 192 camera (which weighs approximately one ton) must sit on the floor of the range access tunnel.

The arrangement intended for shock-wave studies was basically the same as that illustrated in Fig. 8 (and with the additions noted above). The light source, of course, was modified to produce light pulses of approximately 80- $\mu$ sec duration. An auxiliary optical system consisting of a condenser arrangement of a pair of lenses plus a circular knife edge aperture was added in front of the camera lens to enhance flow visualization (schlieren effect) for this application.

### 3.5 PHOTOGRAPHIC RESULTS

The high-speed photographic system was used quite successfully during snow erosion tests. The resulting sequences of photographs provided, as desired, excellent depictions of snowflake/shock wave interactions.

A typical single-frame photograph from an 82-frame record obtained during one of these applications is shown in Fig. 9. Camera framing rate in this instance was 514,000 fps; the corresponding exposure time per frame was  $0.49 \mu\text{sec}$ . Model velocity was 12,000 ft/sec, and the ambient range pressure was 304 torr.

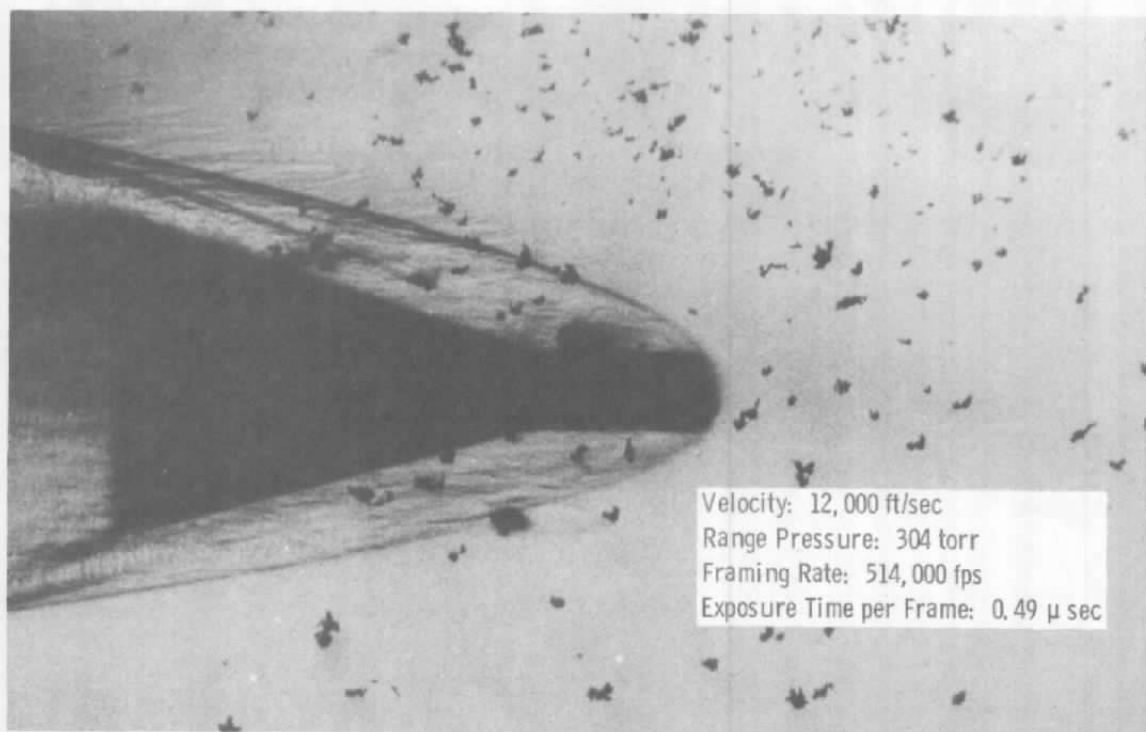
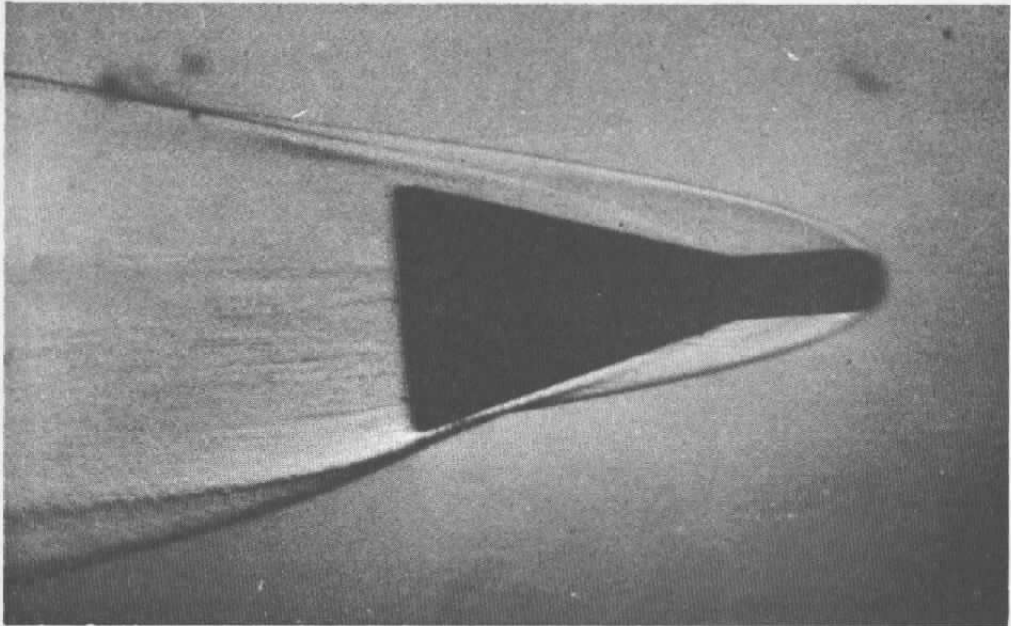


**Figure 9. Typical frame from high-speed photography system, snow erosion studies.**

Launches of model shapes of interest for oscillating shock wave studies have not been made to this date. It was necessary then to evaluate the applicability of the high-speed photographic system for these purposes during other Range G launches. Figure 10 shows a single frame photograph from a sequence obtained during a launch of a test model similar to that depicted in Fig. 9. The model velocity in this case was 18,500 ft/sec and the range pressure was 200 torr. Camera operating speed was 959,000 fps; exposure time per frame was  $0.26 \mu\text{sec}$ . This photograph provides (as do others in the sequence) reasonably good visibility of the bow shock wave except in the immediate vicinity of the nosetip.

The bow shock wave on a blunt model such as the one in the photograph (Fig. 10) does not oscillate to a discernible degree; whereas,



Model Velocity: 18,500 ft/sec  
 Range Pressure: 200 torr  
 Framing Rate: 959,000 fps  
 Exposure Time per Frame: 0.26  $\mu$  sec

**Figure 10.** Typical frame from high-speed photography system, flow visualization mode.

for the model shapes of interest for future studies, shock wave oscillations with amplitudes of as much as one-half inch might be common. One can speculate that, for such cases of large-amplitude oscillations, excursions of readily visible portions of the shock wave may be observed well enough to characterize the phenomena of interest.

#### 4.0 MUZZLE-ZONE/TRACK DETECTOR SYSTEMS

Almost every aeroballistic range instrumentation system requires some means for detecting and annunciating the arrival of the test model at the particular measurement station; i. e. , a properly timed trigger pulse must be provided to activate each system. It was an objective of research work to develop reliable model detection techniques for application in high-luminosity environments. The extremely bright muzzle flash has long plagued efforts to achieve reliable triggering in the blast tank areas of the VKF ranges; also, the Range K and Range G guided track systems are expected to present requirements for model detection in the presence of high ambient light levels.

## 4.1 SYSTEM DESCRIPTION

A detector system employing a He-Ne, continuous-wave laser and a photodiode/integrated circuit package was designed. The system, schematized in Fig. 11, is arranged so that when a model breaks a light beam between the laser and photodiode, an electrical trigger pulse is generated.

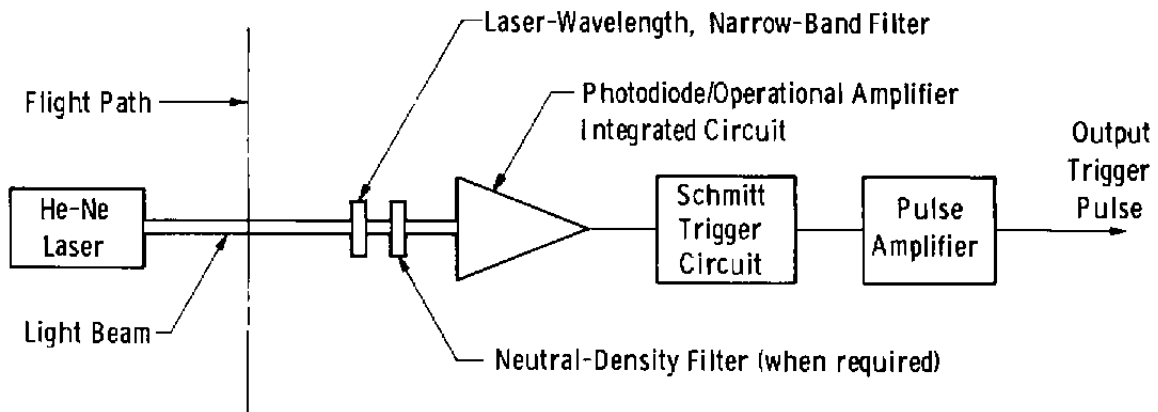


Figure 11. Detector system schematic.

The basic component of the detector system is the integrated circuit package (Bell and Howell, Type 509-01) consisting of a silicon photodiode and high-speed operational amplifier. The device responds to light in the 0.5- to 1.0- $\mu\text{m}$  spectral region and produces a 0- to 10-v output, linearly proportional to the incident radiation intensity over a certain intensity range. The response time of the integrated circuit package is approximately 1  $\mu\text{sec}$ . An interference filter is used to prevent light other than that at, and very near, the laser wavelength (0.6328  $\mu\text{m}$ ) from reaching the photodiode. A neutral-density filter is employed in some cases to further control the amount of light reaching the photodiode. A Schmitt trigger circuit and a pulse amplifier complete the system.

## 4.2 OPERATIONAL CHARACTERISTICS

It was determined that an input of approximately 3 milliwatts of laser light produces an output of approximately 10 v from the integrated circuit (operational amplifier). This "full-scale" output is the desired bias level for the integrated circuit. The output of the integrated circuit is fed into a Schmitt trigger circuit designed to have upper and lower trip points of approximately 6 and 4 v, respectively. Thus, when blockage of the laser beam occurs and the output of the operational

amplifier (input to the Schmitt trigger) drops downward through the 4-v level, the Schmitt trigger circuit produces an output pulse. This operational feature helps to minimize premature triggering which might result from partial interruption of the laser beam by debris particles, muzzle gases, etc\*. Finally, the Schmitt trigger output pulse is amplified to 30-v amplitude, the level typically required for triggering instrumentation systems.

In applications where 3-mw lasers are used with the detector system, proper bias of the integrated circuit is achieved without a neutral-density filter. Other applications, in which higher laser power is used, require use of neutral-density filtering (see Fig. 11) to maintain a 3-mw input to the photodiode for proper bias conditions.

When ambient sources are particularly strong emitters at the laser wavelength (0.6328  $\mu\text{m}$ ), it is necessary to increase the power of the laser used. Obviously, if, during operation, an ambient source contributes 3 mw or more to the total light reaching the photodiode through the wavelength-selective filter (Fig. 11), the detector will remain biased and will not trigger even if the laser beam is blocked. In these cases then, one must choose a laser with power somewhat higher than this laser-wavelength "noise" from the ambient light. A neutral-density filter can then be used to reduce the level of laser light to 3 mw at the photodiode; the filter will, in turn, reduce the "noise" to a level that will not maintain bias of the detector, provided of course that a sufficient differential between laser power and "noise" power has been chosen.

### 4.3 EVALUATIONS

A detector system utilizing a 5-mw laser was evaluated in Range G as a detector for an X-ray shadowgraph system (Ref. 4) located approximately 14 ft from the muzzle. Trigger reliability at this particular location with previously employed detection schemes was on the order of 50 percent. The new detector system was found to afford a trigger reliability of about 80 percent. These initial experiments indicated that increasing the laser power (allowing rejection of more of the unwanted radiation) should increase reliability still further.

---

\*Second-generation detector systems are envisioned in which logic will be applied to the length of the integrated-circuit output pulses to aid further in discrimination against extraneous interruptions of the laser beam.

A system employing a 15-mw laser was used in Hyperballistic Range (K) to trigger a blast-tank X-ray shadowgraph located two feet from the muzzle. During this evaluation, correct triggering was achieved on 12 of 13 shots for a reliability of approximately 93 percent. Previously, for triggering this close to the muzzle, it was necessary to use microwave barrier techniques that were about 70 percent reliable.

Systems with 3-mw lasers were used to trigger laser photography systems (Refs. 1, 4, 5, and 7) and X-ray shadowgraphs during initial shots in the Range K guided-track facility. To date, the detectors have proved to be extremely reliable for these purposes; however, because only a small number of shots have been monitored and only low luminosity levels have been encountered thus far, a numerical value for reliability has not yet been assigned for these systems. In fact, further evaluations, made under more severe conditions, may indicate that higher power lasers are required for acceptable reliability for the track application.

It is felt that the laser detector technique, per se, has been proved for application in high-luminosity environments; the power of the laser for individual systems must be chosen commensurate with the severity of the environment.

## 5.0 CONCLUDING REMARKS

Research efforts have resulted in the development of instrumentation systems that contribute significantly toward improvement of the testing capabilities of the VKF aeroballistic ranges for both free-flight and guided-track modes of operation.

New areas of testing have been entered in Range G as a result of the development of a photographic pyrometry instrumentation system capable of model surface temperature measurements as low as 1,900 K. Successful applications of the "low" temperature photopyrometer were made possible by complementary implementation of a dual-environment technique for circumventing problems associated with shock-cap radiation.

The new photopyrometry system proved to be quite useful for providing important qualitative data, namely, photographic depictions of luminous wakes behind certain test models. This basic ability of the system to record low-level, self-luminosity events will no doubt be exploited in other test areas.

Erosion testing capability has been enhanced by development of the ability to acquire movie-like sequences of photographs of models in flight within erosive environments. These data allow studies of the interactions of individual erosion particles and model flow fields.

The high-speed photography system shows promise for application during future studies of oscillating shock waves on certain test models. Thorough evaluation of the system for this purpose must await launches of models more nearly simulating the nosetip shapes of interest.

The newly developed detector systems have certainly improved model detection capability within the blast-tank areas of Ranges G and K. These types of detectors will be applied extensively in the future for triggering instrumentation systems in the Range K and Range G guided-track facilities. It is felt that they will perform equally well for all shot conditions, thus eliminating the need for separate "shadow" and "luminosity" operational modes characteristic of ballistic range detection systems.

#### REFERENCES

1. Dugger, P. H. "Optical Instrumentation Studies in Aerospace Facilities -- A Project Summary." AEDC-TR-72-141 (AD750866), October 1972.
2. Dugger, P. H., et al. "Photographic Pyrometry in an Aeroballistic Range." Proceedings of the SPIE 16th Annual Technical Meeting, San Francisco, California, October 1972.
3. Dugger, P. H., et al. "A High-Speed Photographic Pyrometer." Proceedings of the Electro-Optics '71 East Conference, New York, September 1971.
4. Hendrix, R. E. and Dugger, P. H. "Photographic Instrumentation in Hyperballistic Range (G) of the von Kármán Gas Dynamics Facility." Photographic Applications in Science, Technology and Medicine, Vol. 8, No. 5, September 1973.
5. Norfleet, G. D., Hendrix, R. E., et al. "Development of an Aeroballistic Range Capability of Testing Re-Entry Materials." Proceedings of the AIAA 8th Aerodynamic Testing Conference, Bethesda, Maryland, July 1974.

6. Kingslake, Rudolph, Ed. Applied Optics and Optical Engineering  
Volume I, Light: Its Generation and Modification.  
Academic Press, New York, 1965.
7. Dugger, P. H. and Hendrix, R. E. "Laser Photography: A Role  
at the AEDC." Optical Spectra, Vol. 9, No. 5, May 1975.